COMPARISON OF OPTICAL AND SAR DATA IN TROPICAL LAND COVER CLASSIFICATION FOR REDD+

Laura Sirro (1), Tuomas Häme (1), Yrjö Rauste (1), Oleg Antropov (1), Jarno Hämäläinen (2), Petri Latva-Käyrä(2), Fernando Paz (3), Bernardus de Jong (4)

(1) VTT Technical Research Centre of Finland, P.O. Box 1000, FI-02044 VTT, Finland, laura.sirro@vtt.fi
(2) Oy Arbonaut Ltd., Kaislakatu 2, FI-80130 Joensuu, Finland, jarno.hamalainen@arbonaut.com
Latokartanontie 7 A, FI-00700 Helsinki, Finland, petri.latva-kayra@arbonaut.com
(3) Colegio de Postgraduados, Km 36.5 Carretera México-Texcoco, 56230 Texcoco, México, pellat@colpos.mx
(4)El Colegio de la Frontera Sur, Av. Rancho Polígono 2A, Parque Industrial Lerma
Campeche, Campeche, CP 24500, México, bjong@ecosur.mx

ABSTRACT

A comparison study was performed to evaluate the applicability of optical and SAR data for land cover classification for REDD+ services on a test site in Chiapas State in Mexico. The accuracy of the maps was assessed using an independent data set that was collected from very high resolution optical data.

The overall accuracy of the maps varied between 79 % of ENVISAT ASAR and 94 % of RapidEye for the forest – non-forest classifications. The accuracies for the six IPCC compliant classes were from 5 to 9 percentage units lower. Results that were obtained with the optical data were somewhat better than the results using the SAR data. However, the difference between the optical and SAR results was fairly small when L-band SAR data were used. L-band SAR data seem to be competitive alternative for optical data particularly in the areas with frequent cloud cover.

1. INTRODUCTION

The Measurement, Reporting and Verification (MRV) activity of the REDD+ (Reducing Emissions from Deforestation and Forest Degradation) process requires reliable and robust methods for the assessment of land cover classes and their changes. Remote sensing based services can fulfil many of the requirements of the MRV services. However, the lack of both ground reference data and Earth Observation (EO) data often complicates the provision of earth observation based services. Optical EO data are frequently contaminated by clouds which make SAR (Synthetic Aperture Radar) imagery an attractive data source. The REDD+ services would benefit from using several alternative image types.

Research projects have reported variable accuracies that are based on different approaches in image interpretation and accuracy assessment. Such variability makes it difficult to evaluate the robustness and performance of the approaches and different data sources. Accuracy assessment approaches that are based on VHR (Very High Resolution) optical images can be implemented globally. Such approach was applied in this study. The methodology that was used is described in [1].

To evaluate the applicability of different EO data sources for forest monitoring services for REDD+ a comparison study was performed. Five land cover classifications were compiled using RapidEye, Landsat TM, ENVISAT ASAR and ALOS PALSAR data. The accuracy of the maps was assessed independently from the classification using a data set that was collected using VHR data.

2. MATERIALS AND METHODS

2.1. Study site and class definition

The study was performed in a site of approximately 100 km by 100 km in the Eastern part of the State of Chiapas in Mexico (Fig. 1).

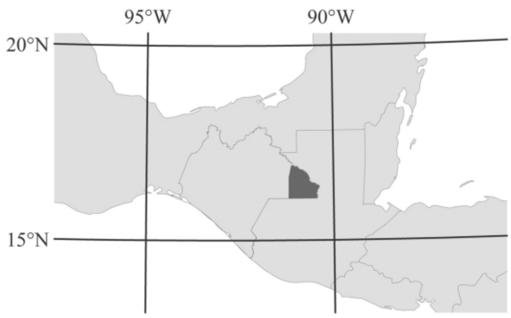

Figure 1. The location of the study site.

Six land use classes that are compatible with the good practice guidance [2] of IPCC (Intergovernmental Panel on Climate Change): 'forest land', 'cropland', 'grassland', 'wetlands', 'settlements' and 'other land' were used in the accuracy assessment of the classifications. Additionally, a class 'shrubland' was

Proc. 'ESA Living Planet Symposium 2013', Edinburgh, UK
9–13 September 2013 (ESA SP-722, December 2013)

used in the classification. In the accuracy assessment 'shrubland' class was included in the 'grassland' class. For forest, the FAO thresholds, forest cover larger than 10 percent and minimum height 5 meters [3], were used.

2.2. Very high resolution optical and ancillary data

The reference data were collected from eight very high resolution satellite images. Level 1G Kompsat-2 images from years 2008-2011 were received through European Space Agency (ESA) Category-1 project C1P.1519 (Tab. 1). The pixel size of the images was one meter on the panchromatic band and four meters on the multispectral bands.

Google Earth was used as an additional information source on land cover and image geometry. Google Earth was the best available data for the geographic reference.

Table 1. Kompsat-2 images that were used in the study.

Acq. Date	Orbit	Frame
29 JUL 2008	24825	1123
29 JUL 2008	24285	1125
11 MAY 2008	09643	1122
02 JUN 2010	20529	1120
10 MAR 2010	19302	1124
10 MAR 2010	18966	1129
23 MAR 2010	19492	1122
23 MAR 2011	24825	1121

Aster DEM (Digital Elevation Model) [4] was downloaded from http://gdem.ersdac.jspacesystems.or.jp/search.jsp and used in the pre-processing of the SAR data.

2.3. Wall-to-wall EO data

Thirteen level 3A RapidEye images were used. The size of each tile was 25 km by 25 km. The images had been acquired between May and September 2009 (Tab. 2). They were available from Mexico in WGS84 datum and UTM projection (zone 15, northern hemisphere) as all the data that were used in the study.

Table 2. The dates of the RapidEye tiles used.

Acq. Date	Number of images
25 MAY 2009	1
13 JUN 2009	1
21 JUL 2009	9
13 SEP 2009	2

Two Landsat TM level 1T (Standard Terrain Correction) images that had been acquired 9.12.2009 (path: 20, row: 48-49) were ordered from the USGS archives (http://earthexplorer.usgs.gov/). The aim of the data procurement was to select the most cloud free Landsat TM images from year 2009. Even the selected images had quite an extensive cloud cover.

Twenty-eight ENVISAT ASAR images were received through ESA Data Warehouse. The images were image mode data from swath IS2 (mid-swath nominal incidence angle 23 degrees). Two image frames were required to cover the area to be mapped. For one of the frames ASAR scenes from six different dates and for the other from five dates were available. Scenes were screened visually, and those scenes that had poor contrast between forest and fields were left out from further processing. Tab. 3 lists the remaining ASAR scenes. Thus after the image selection part of the site had four overlapping images and the other part three.

Table 3. ASAR scenes that were used in the study.

Acq. Date	Time (UTC)	Latitude	Longitude
08 MAR 2004	16:03:01	15.967	-91.005
12 APR 2004	16:02:59	15.967	-91.011
17 MAY 2004	16:03:02	15.964	-91.004
13 MAR 2006	16:02:51	15.966	-91.002
08 MAR 2004	16:02:46	16.853	-90.816
17 MAY 2004	16:02:47	16.849	-90.816
13 MAR 2006	16:02:36	16.852	-90.814

ALOS data consisted of eighteen dual-polarised PALSAR scenes that were acquired in years 2007, 2008, and 2009. They were received through ESA Category-1 project C1P.6213.

2.4. Data processing

2.4.1. Visual interpretation of VHR data

The geometry of the Kompsat-2 images was compared visually to the RapidEye data and additional corrections were performed using ground control points measured between the RapidEye data and the Kompsat-2 images. Pan-sharpening was applied to compile the images for the visual interpretation.

A grid of square shaped plots of 50 meters by 50 meters with 800 meters interval in both northing and easting direction was created for each VHR image. The total number of plots was 1680. For the plots the proportion of each land cover class was defined visually using a GIS software.

The plots were divided into two sets, one for the training and another for the accuracy assessment. The division into the two data sets was done by the geographic location of the plots. Two different division options were applied: North-South division and East-West division. For each VHR image and for the both division types, the land cover statistics of the two resulting datasets were compared. The division which created the most similar land use statistics between modelling and test set was chosen. Based on random selection, one of the two datasets per image was assigned for the training and the other one for the accuracy assessment. Only the training data set was made available for the compilation of the classifications. The project partner who collected the reference data was not involved in the classification and kept the other data set for the accuracy assessment.

The plot data set was forest-dominated. The proportion of the forest area was 73 % when unstocked forest areas were not included in this percentage.

2.4.2. Pre-processing of wall-to-wall data

Optical

RapidEye level 3A orthoproduct was used, which means that the data had already been ortho-rectified before distribution. The co-alignment of some image tiles in the data set required additional adjustment. This was done using block adjustment [5] and ground control points measured from the data and Google Earth. The data were received with five meter pixel size. Because of the classification method that was based on using the individual pixel values the data were averaged to ten meter pixel size.

Atmospheric correction was performed for all the RapidEye tiles using SMAC (Simplified Method for Atmospheric Correction) [6]. An additional offset calibration of the reflectance values using MODIS data was applied. The red edge band of RapidEye data was excluded from the further processing because the MODIS data that would have been required for the offset calibration were not available for the wavelength. A cloud mask was created manually using a GIS software.

For the Landsat TM data no additional geometric correction was required but the data were resampled from 30 to 25 meter pixel size. SMAC atmospheric correction was performed but additional calibration was not necessary since the images were from the same date and originally very similar. Also for the Landsat images the cloud mask was created manually.

SAR

ALOS/PALSAR HH and HV bands were pre-averaged in the power domain over seven lines (averaging along track in a constant range bin). All scenes were ortho-rectified and radiometrically corrected individually. Bilinear interpolation was used in the pixel resampling. The pixel spacing of the ortho-rectified PALSAR scenes was set to 25 m. Yearly mosaics were compiled separately for the HH and HV bands. A visual check was done for the year-to-year co-registration. No signs of co-registration problems were noticed at the boundaries of the neighbouring scenes. The data were compared to Google Earth and as a result all PALSAR scenes were shifted 55.6 m south in the final ortho-rectification and the mosaics were re-compiled.

After the pre-processing, average amplitude and temporal variability (standard deviation of the logarithm of backscatter amplitude) features were computed using the mosaics from all the years. Visual analysis of the feature images revealed that the original amplitude bands separated the classes better. Finally, the HH and HV amplitude mosaics 2009 were selected for the classification.

The ASAR scenes were ortho-rectified [7] and radiometrically corrected using Aster DEM, tie points between scenes, and ground control points between the scenes and Google Earth. The ASAR scenes were down-averaged to 50 meter pixel spacing to reduce noise. Mean backscatter amplitude and temporal variability were computed for each pixel and used as inputs for the classification.

2.4.3. Classification of wall-to-wall data

Land cover maps with six classes were produced using all the data sets except ENVISAT ASAR data. For the ENVISAT ASAR data only a forest – non-forest map was compiled, because the separation of the six classes appeared unsuccessful in the preliminary testing.

An iterative classification approach was applied. The training plots of each VHR image were divided into two subsets, A and B. First only the set A was used in the classification and a land cover map was compiled. When a sufficient training accuracy was reached using the set A, the set B was introduced. The classification was then fine-tuned using the set B. The aim of the iterative approach was to make it possible to follow how the accuracy and the commission and omission errors develop when more data are introduced. The main criterion for an acceptable result was to maximize the classification accuracy and to minimize the difference between the omission and the commission errors of the resulting maps for the training data.

Land cover classification was done using the probability method [8]. The selected image area was first classified with unsupervised k-means clustering. For each cluster, the proportion of land cover classes was defined using the reference data. If no ground reference data were available for a cluster its land cover class proportions were defined with the help of other available information, e.g. Google Earth. Finally, the estimates for the proportion of each land cover class were computed for every pixel in the image using the statistics and the ground data contents of the cluster classes. The land cover maps were compiled from the continuous estimates of each land cover class proportion using a hierarchical approach. First, the pixel was classified as forest if the forest proportion estimate was higher than non-forest estimate of that pixel. Otherwise the pixel was classified as non-forest. After that the non-forest pixels were classified to the dominating non-forest class.

The same classification approach was used for all the data sources but for different data sources different post-processing approaches were applied. For the optical data an additional mask was created for the water areas. It was included in the 'wetlands' class. As a post processing of the SAR based land cover maps majority filtering was applied. The aim was to reduce the effect of speckle. For the land cover maps using PALSAR data, 3 by 3 pixel (75 m by 75 m) majority filter was shown to be useful and it was applied to the final map. For ASAR classifications majority filtering in a 5 by 5 pixel (250 m by 250 m) window was applied.

ASAR data were used for improving the separation of the class 'settlement' in the PALSAR classification. If a pixel's 5-by-5 neighbourhood included at least 3 pixels classified as 'settlement' in the ASAR classification the pixel was classified as 'settlement' in the map. If a pixel classified as 'settlement' was within 1 km from the closest steep, lay-over producing slope, in the ASAR data the pixel was given the class according to the PALSAR classification.

The maps that were produced for the accuracy assessment are listed in Tab. 4. In addition of the maps made using each data type, a map where all the maps were combined was created. The maps that were compiled using optical data were augmented in the cloudy regions with maps that were made using SAR data. The maps were used in the order of the overall accuracy so that the map with the highest accuracy was on the top of the stack of the maps.

Table 4. The produced land cover maps.

Map	Data
A	RapidEye
B	Landsat TM
C	ALOS PALSAR
D	ENVISAT ASAR (forest – non-forest)
E	ENVISAT ASAR, ALOS PALSAR
F	Combination of the classifications from RapidEye, Landsat TM, ALOS PALSAR and ENVISAT ASAR

2.4.4. Accuracy assessment

For each plot in the test data set from the visual interpretation the corresponding class was extracted from the classified maps. Both the classes in the reference data and the classes in the maps were aggregated to the six IPCC classes. If more than 10 % of the validation plot area was covered by unclassified pixels in the map (clouds, no data), the plot was excluded from the accuracy assessment.

From the extracted data set a confusion matrix was created for each map. Overall accuracy for the six IPCC compatible classes and the overall accuracy for the forest – non-forest classification were computed. In addition, the user's and producer's accuracies and the omission and commission errors were computed from the confusion matrices.

3. RESULTS

The resulting maps are shown in Figure 22 and Tab. 5 summarizes the results from the accuracy assessment. The overall accuracy of the maps varied between 79 % of ENVISAT ASAR and 94 % of RapidEye for the forest-non forest classifications and between 81 % of ENVISAT ASAR and ALOS PALSAR and 86 % of RapidEye when the six IPCC classes were used.

The omission errors for the forest class varied from 6 % of the combination map to 15 % of ENVISAT ASAR and commission errors from 2 % of RAPIDEYE to 13 % of ENVISAT ASAR. The largest bias (5 %) was in the RapidEye classification where the overall classification accuracy was the highest. It may be caused by overtraining of the model.

The confusion matrices (Tab. 6 - Tab. 8) show that in the six class classification using both optical and SAR data sets 'grassland' and 'cropland' classes were mixed to a large extent. 'Wetlands' class was separated well using optical data. For 'settlements' and 'other land' class there was a lack of reference data.

In the Landsat images the non-cloudy area was 51 % and in the RapidEye data 87 %, respectively. For SAR data sets the whole area of the images was mapped. The number of observations that were used for the accuracy assessment was consequently lower for the optical data.

The combined use of PALSAR and ASAR data did not improve the accuracy. However the 'settlements' class was better separated in the map that was produced by combining PALSAR and ASAR data than in the map that was made using only PALSAR data. When all the maps were combined, the accuracy for the forest and non-forest classification was 94 % and for the six classes 85 %. The omission error for the forest class was 6 % and the commission error 3 %.

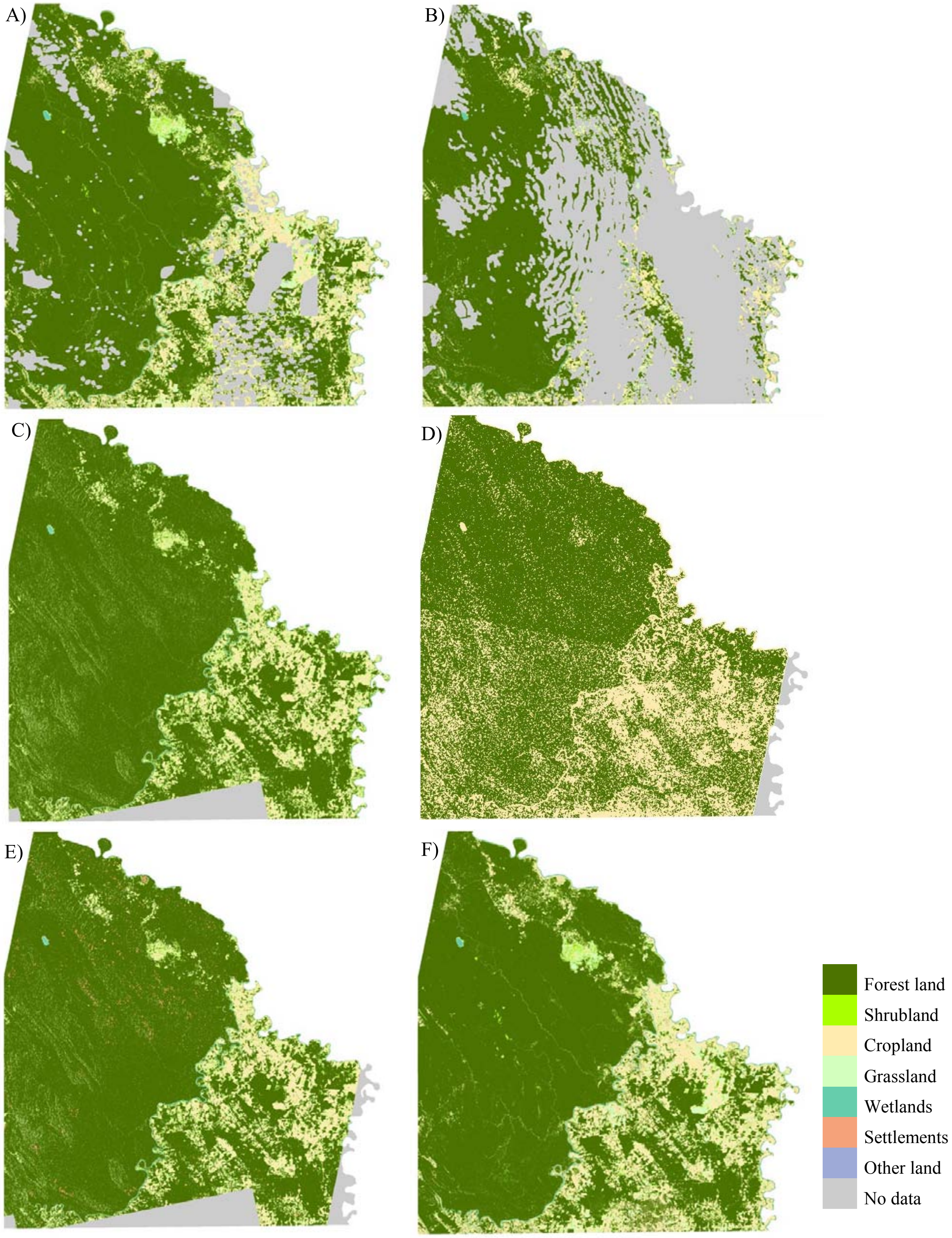

Figure 2. The land cover maps produced using different source data sets: A) RapidEye, B) Landsat TM, C) ALOS PALSAR, D) ENVISAT ASAR, E) ALOS PALSAR and ENVISAT ASAR and F) Combination of the maps.

Table 5. The results of the accuracy assessment: A) RapidEye, B) Landsat TM, C) ALOS PALSAR, D) ENVISAT ASAR, E) ALOS PALSAR and ENVISAT ASAR and F) Combination of the maps.

Map	Overall accuracy (forest non-forest)	Overall accuracy (six classes)	Omission error for forest class	Commission error for forest class	Num. obs.	Proportion of the mapped area from the whole test area
A	94 %	86 %	7 %	2 %	704	87 %
B	91 %	86 %	7 %	5 %	392	51 %
C	89 %	82 %	6 %	8 %	805	98 %
D	79 %	-	15 %	13 %	798	96 %
E	89 %	81 %	7 %	8 %	765	95 %
F	94 %	85 %	6%	3 %	840	100 %

Table 6. Confusion matrix for the RapidEye classification with the six IPCC compliant classes.

		Reference							
		Forest land	Cropland	Grassland	Wetlands	Settlements	Other land	Total	User's acc.
Map	Forest land	485	0	10	0	0	0	495	98 %
	Cropland	20	94	32	0	0	0	146	64 %
	Grassland	14	23	13	0	0	0	50	26 %
	Wetlands	0	1	0	11	0	1	13	85 %
	Settlements	0	0	0	0	0	0	0	na
	Other land	0	0	0	0	0	0	0	na
	Total	519	118	55	11	0	1	704	
	No data	95	29	12	0	0	0	136	
	Prod. acc.	93 %	80 %	24 %	100 %	na	0		86 %

Table 7. Confusion matrix for the ALOS PALSAR classification with the six IPCC compliant classes.

		Reference							
		Forest land	Cropland	Grassland	Wetlands	Settlements	Other land	Total	User's acc.
Map	Forest land	554	16	33	1	0	0	604	92 %
	Cropland	12	87	16	0	0	1	116	75 %
	Grassland	25	37	12	2	0	0	76	16 %
	Wetlands	1	0	0	8	0	0	9	89 %
	Settlements	0	0	0	0	0	0	0	na
	Other land	0	0	0	0	0	0	0	na
	Total	592	140	61	11	0	1	805	
	No data	22	7	6	0	0	0	35	
	Prod. acc.	94 %	62 %	20 %	73 %	na	0		82 %

Table 8. Confusion matrix for the combination of the maps with the six IPCC compliant classes.

		Reference							
		Forest land	Cropland	Grassland	Wetlands	Settlements	Other land	Total	User's acc.
Map	Forest land	576	0	16	0	0	0	592	97 %
	Cropland	25	115	35	0	0	0	175	66 %
	Grassland	12	32	16	0	0	0	60	27 %
	Wetlands	1	0	0	11	0	1	9	85 %
	Settlements	0	0	0	0	0	0	0	na
	Other land	0	0	0	0	0	0	0	na
	Total	614	147	67	11	0	1	840	
	No data	0	0	0	0	0	0	0	
	Prod. acc.	94 %	78 %	24 %	100	na	0		85 %

4. SUMMARY AND CONCLUSIONS

Accuracies that were obtained using optical data were higher than those that were obtained using SAR data. The difference in the forest non-forest classification results was fairly small when ALOS PALSAR data were used. More research on the potential of SAR data in land cover classification is required since in a similar study that was performed on a study site in Laos [1] the results with L-band SAR were poorer. However, the results of the current study indicate that the land cover maps made using optical and L-band SAR can be used to complete each other in forest – non-forest classification.

In the case of six IPCC compliant classes it was not possible to reliably separate the classes ‘grassland’ and ‘cropland’ from each other using any of the used data sets. This is likely because the vegetation in the two land use types is very similar and they are difficult to separate using data from single date.

The results obtained using ENVISAT ASAR data in this study were modest. Many earlier studies have shown that forest vs. non-forest mapping in tropical areas with C-band radar data require data acquired during dry conditions. The ASAR dataset used here may not have included enough good scenes acquired in dry conditions. The ASAR dataset also consisted of IS2 data with a steep incidence angle of 23 degrees. Forest non-forest discrimination is better with data from beam modes with higher incidence angles [9]. Study of the data catalogues showed that IS2 data were the most common beam mode in the study site leading to the highest number of observations for temporal variability. Therefore, IS2 data were selected for use in the study.

ACKNOWLEDGEMENT

The research leading to these results has received funding from the European Union Seventh Framework Programme (FP7/2007-2013 – ReCover) under grant agreement n° 263075.

The authors wish to thank the European Space Agency (ESA) for the provision of the Kompsat-2 and ALOS PALSAR images under Category-1 Projects (C1P.1519 and C1P.6213).

REFERENCES

1. Häme, T., Kilpi, J., Ahola, H., Rauste, Y., Antropov, O., Rautiainen, M., Sirro, L. & Bounpone, S. (2013). Improved mapping of Tropical forests with optical and SAR imagery, Part I: Forest Cover and Accuracy Assessment Using Multi-Resolution Data. IEEE Journal of Selected Topics in Applied Earth Observations and Remote Sensing, vol. 6, 1, pp.74-91.

2. IPCC (2003). Good Practice Guidance for Land Use, Land-Use Change and Forestry. Institute for Global Environmental Strategies (IGES).

3. FAO (2000). On definitions of forest and forest change. Forest Resources Assessment Programme, Working Paper 33. FAO, Rome, Italy. 15 p.

4. Tachikawa, T., Hato, M., Kaku, M., & Iwasaki, A. (2011). The characteristics of ASTER GDEM version 2. Geoscience and Remote Sensing Symposium (IGARSS), July 2011.

5. De Grandi, G., Mayaux, P., Rauste, Y., Rosenqvist, Å., Simard, M., & Saatchi, S. (2000). The global rain forest mapping project JERS-1 radar mosaic of tropical Africa: Development and product characterization aspects. IEEE Transactions on Geoscience and Remote Sensing, Vol. 38, No. 5, September 2000, pp. 2218-2233.

6. Rahman, H., & Dedieu, G. (1994). SMAC: a simplified method for the atmospheric correction of satellite measurements in the solar spectrum. International Journal of Remote Sensing, vol 15, pp. 123–143.

7. Rauste, Y., Lönnqvist, A., Molinier, M., Henry, J-B., & Häme, T. (2007). Ortho-Rectification and Terrain Correction of Polarimetric SAR Data Applied in the ALOS PALSAR Context. Proc. Int. Geoscience and Remote Sensing Symp., Barcelona, Spain, 23.-27.7.2007, pp. 1618 - 1621.

8. Häme, T., Stenberg, P., Andersson, K., Rauste, Y., Kennedy, P., Folving, S., & Sarkeala, J. (2001). AVHRR-based forest proportion map of the Pan-European area, Remote Sensing of Environment, vol. 77, pp. 76-91.

9. Rauste, Y., Häme, T., Ahola, H., Stach, N., & Henry, J.-B. (2007). Detection of forest changes over French Guiana using ERS-1 and ASAR imagery. Proceedings of Envisat Symposium 2007, ESA SP-636, European Space Agency. Noordwijk, The Netherlands.